JARQ 57 (1), 73-77 (2023) https://www.jircas.go.jp

Suspected Case of MALT Lymphoma of the Nasal Turbinate in a Horse

Daiki KAWASHIMA[1], Osamu MIKAMI[2]*, Tomoyuki SHIBAHARA[3], Yoshiharu ISHIKAWA[2] and Koichi KADOTA[2]*

[1] Matsumoto Livestock Hygiene Service Center, Matsumoto, Japan
[2] Sapporo Research Station, National Institute of Animal Health, National Agriculture and Food Research Organization, Sapporo, Japan
[3] Kagoshima Research Station, National Institute of Animal Health, National Agriculture and Food Research Organization, Kagoshima, Japan

Abstract

We examined a female Kiso horse (a native Japanese horse breed) aged 2 years and 9 months with persisting nasal discharge that died due to lymphoma. Necropsy revealed masses in the left nasal cavity, left periorbital cavity, and left maxillary and mandibular areas. Histologically, the neoplastic tissues were composed of lymphoid and plasmacytoid cells, with immunoglobulin A (α and λ chains) production in the latter. The foci of large lymphoid cells were detected at some sites. All neoplastic cell types were positively stained in immunohistochemical staining for CD20. Extranodal marginal zone B-cell lymphoma of mucosa-associated lymphoid tissue (MALT lymphoma) was suspected on the basis of the presence of lymphoepithelial lesions, plasmacytic differentiation, and large-cell transformation. A history of chronic rhinitis may be linked to the development of this disorder.

Discipline: Animal Science
Additional key words: Extranodal marginal zone B-cell lymphoma, large-cell transformation, lymphoepithelial lesion, plasma cell differentiation

Introduction

Reports of lymphoid neoplasms in horses are relatively common, and most cases are in multicentric form (Jacobs et al. 2002). The next most frequent form is alimentary, whereas thymic and skin (epitheliotropic) forms are rare (Jacobs et al. 2002). Solitary lymphomas at extranodal sites have been reported in the third eyelid, tongue, urinary bladder, ovary, and leg (Muñoz et al. 2009, Miglio et al. 2019). In a histological study of multiple cases of lymphoma, the common subtypes were T-cell-rich large B-cell lymphoma, peripheral T-cell lymphoma, and diffuse large B-cell lymphoma (Durham et al. 2013).

Human MALT lymphoma is a low-grade B-cell lymphoma derived from the post-germinal center and marginal zone B-cell (Isaacson et al. 2008). This lymphoma is histologically characterized by a marginal zone growth pattern or follicular colonization and lymphoepithelial lesions. It may also show plasmacytic differentiation and large-cell transformation (Feller & Diebold 2004a, Isaccson et al. 2008). MALT lymphoma of the neck and head region may occur with chronic inflammation in extranodal organs, such as the ocular adnexa, salivary gland, thyroid gland, and Waldeyer's ring (Wenzel et al. 2003, Hosokawa et al. 2011). In veterinary literatures, marginal zone lymphomas have been usually reported in dogs and have been shown to primarily occur in the spleen or lymph nodes (Valli et al. 2006). In this paper, we describe an equine suspected case of MALT lymphoma that was characterized by lymphoepithelial lesions, plasmacytic differentiation with immunoglobulin A (IgA) production, and cluster formation of large lymphoid cells.

*Co-corresponding authors: mikami@affrc.go.jp, kkadota@affrc.go.jp
Received 4 January 2022; accepted 5 April 2022.

Materials and methods

1. Animal

A female Kiso horse (a Japanese native horse breed) with a history of constitutional weakness and nasal discharge detected soon after birth and persisted throughout the suckling period exhibited protrusion of the left eye and purulent nasal discharge at the age of 2 years and 9 months. Despite nasal lavage and administration of antibiotics and nonsteroidal anti-inflammatory drugs, swelling of the left lower jaw occurred with elevation of the body temperature to 39.5°C 4 days later. In addition, the horse was depressed and anorexic. The animal's condition subsequently remained unchanged, and it died 11 days after the onset of clinical signs. The horse was necropsied, and the tissue samples were collected.

2. Histological and immunohistochemical examination

Tissue samples (liver, spleen, kidney, heart, lung, stomach, cecum, lymph nodes, aorta, pulmonary artery, left eye, left nasal cavity tumor (include nasal turbinate), and maxillary and mandibular tumor (left elevator muscle of the upper lip and depressor muscle of the lower lip)) were fixed in 10% neutral buffered formalin, embedded in paraffin wax, sectioned at 4 µm, and stained with hematoxylin and eosin (HE) and Giemsa. Immunohistochemical analysis was conducted using the streptavidin–biotin complex/horseradish peroxidase (SAB-PO) method on paraffin sections using a commercially available Histofine kit (Nichirei, Tokyo, Japan), rabbit polyclonal antibodies against CD3 (Dako A/S, Glostrup, Denmark), CD20 (Spring Bioscience, Pleasanton, CA, USA), horse IgM (µ chain specific) (Bethyl Laboratories, Montgomery, TX, USA), horse IgG (heavy chain and light chain) (Bethyl), horse IgA (α chain specific) (Bethyl), human κ light chain (Fitzgerald, Acton, MA, USA), and human λ light chain (Fitzgerald). Antigen retrieval was performed *via* enzymatic digestion with 0.05% pepsin at 37°C for 25 min (CD3, IgM, IgG, and IgA). The remnants of normal lymphoid tissues of the lymph nodes were used as internal positive controls, and phosphate-buffered saline was used in place of the primary antibodies for negative controls.

Results

1. Gross pathology

Necropsy revealed a grayish-white intraorbital tumor mass surrounding the left eyeball, with a maximal thickness of 2 cm. The elevator muscle of the upper lip (maxillary area) and depressor muscle of the lower lip (mandibular area) at the left side, which were replaced by white tumor tissues, measured 16 cm × 3 cm × 3 cm and 15 cm × 4 cm × 4 cm, respectively. The left nasal turbinates were replaced by a tumor mass, with almost complete obstruction of the nasal cavity; however, endoturbinates were detectable. The ascending aorta and adjacent pulmonary aorta were extensively covered with white tumor tissues, with a maximal thickness of 4 cm. The left mandibular lymph node was slightly swollen.

2. Histological and immunohistochemical findings

Histological examination revealed similar neoplastic tissues in the macroscopically visible tumor masses, which mainly consisted of small to medium-sized lymphoid or plasmacytoid cells (Fig. 1A, B). In these cells, the nuclei were round, oval, or occasionally irregular with inconspicuous nucleoli and relatively to moderately condensed chromatin. The cytoplasm was scanty or moderately abundant in the lymphoid cells, whereas it was more abundant in the plasmacytoid cells. In some places, large lymphoid cells were scattered or focally accumulated (Fig. 1C) and were characterized by round or oval vesicular nuclei, medium-sized nucleoli, and abundant pale cytoplasm (Fig. 1D) with occasional mitotic figures. In the turbinate mucosa, the mucosal epithelium was invaded by lymphoma cells (lymphoepithelial lesion) (Fig. 1E). In the mandibular, internal iliac, and inguinal lymph nodes, the parenchyma and capsule were slightly or moderately infiltrated by neoplastic cells, and the splenic red pulp was moderately affected. Neoplastic cell infiltration was mild in the hepatic Glisson's capsule, renal stroma, cardiac stroma, peribronchial connective tissue, and abomasal submucosa. In the intranasal, intraorbital, intramuscular (maxillary and mandibular areas), and periaortic tumors, all of the nerve bundles examined were infiltrated by lymphoma cells. The tumor cells were observed beneath the perineurium and in the endoneurium, although neoplastic invasion was not detected in the surrounding fat tissue (Fig. 1F). In the lungs, most alveoli were filled with edematous fluid.

Immunohistochemical evaluations revealed that all types of neoplastic cells were positive for CD20 but not for CD3. In the turbinate mucosa, intraepithelial neoplastic cells also expressed CD20 (Fig. 2A), but some CD3-positive small lymphocytes were admixed with them (Fig. 2B). A large number of CD3-positive lymphocytes were present in the lamina propria. Plasmacytoid cells and some lymphoid cells with moderate amounts of cytoplasm were positive for cytoplasmic IgA (α and λ chains) (Fig. 2C, D). Ig

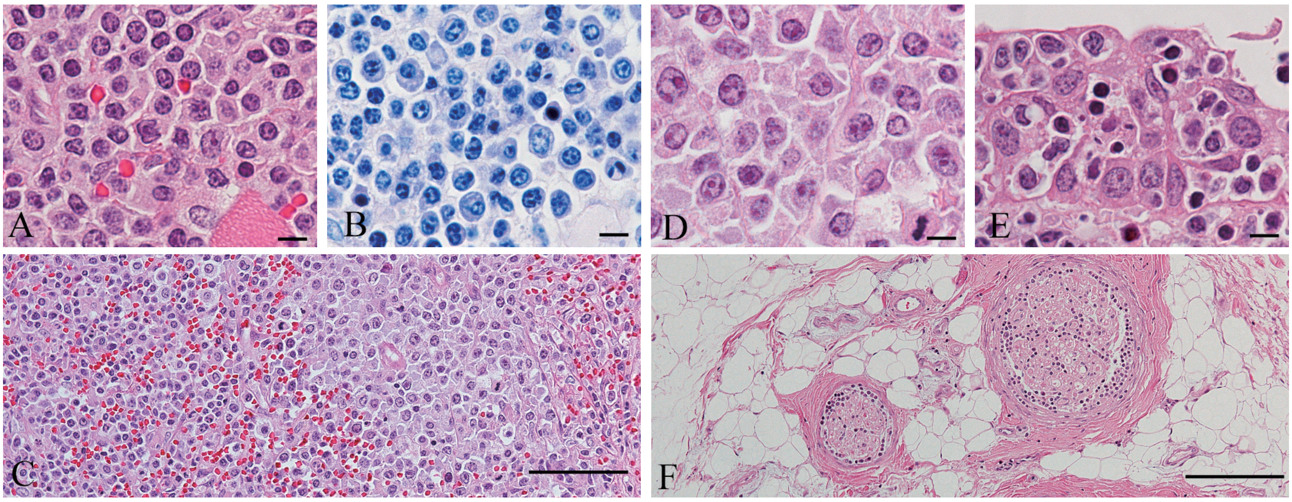

Fig. 1. Histology

(A) Left mandibular tumor: Medium-sized lymphoid cells. HE staining. Bar = 5 µm. (B) Nasal tumor: Small lymphoid cells and plasmacytoid cells. Giemsa staining. Bar = 5 µm. (C) Nasal tumor: Large lymphoid cells form a cluster (right) within neoplastic tissue. HE staining. Bar = 50 µm. (D) Nasal tumor: Cluster in Figure 1C shows large lymphoid cells with abundant cytoplasm. HE staining. Bar = 5 µm. (E) Nasal tumor: The mucosal epithelium is infiltrated by neoplastic cells and lymphocytes. HE staining. Bar = 5 µm. (F) Left mandibular tumor: Neoplastic invasion in the perineurium and endoneurium. HE staining. Bar = 100 µm

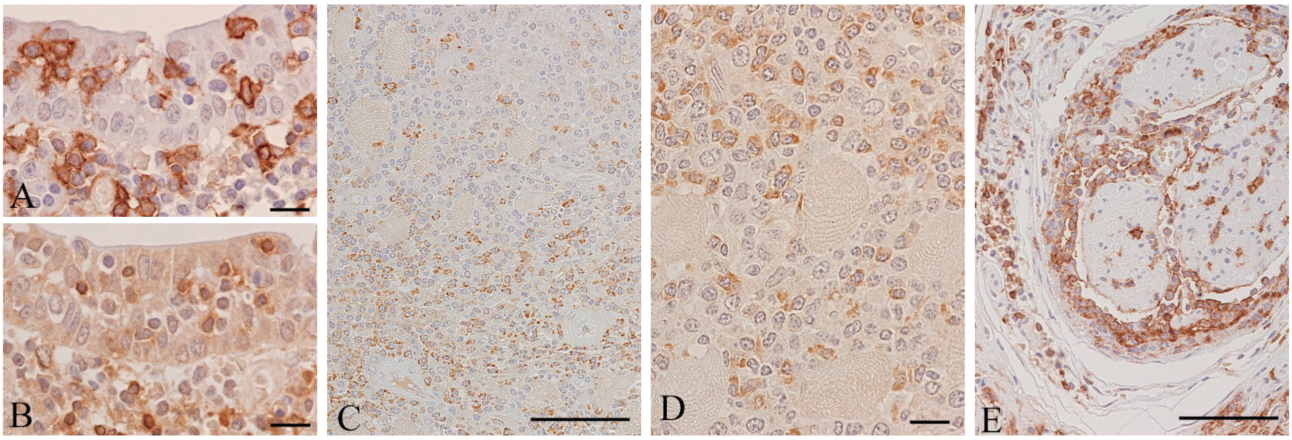

Fig. 2. Immunohistochemistry (IHC)

(A) Nasal tumor: CD20-positive neoplastic cells within and beneath the mucosal epithelium. IHC (CD20). Bar = 10 µm. (B) Nasal tumor: In comparison with the CD20-positive neoplastic cells in Figure 2A, the CD3-positive lymphocytes are smaller in size and number. IHC (CD3). Bar = 10 µm. (C) Left mandibular tumor: Neoplastic cells expressing the λ light chain are inconspicuous in the upper half area where large lymphoid cells predominate. IHC (λ light chain). Bar = 50 µm. (D) Left mandibular tumor: A large number of α heavy chain-positive neoplastic cells, α chain-negative large lymphoid cells, and residual striated muscle cells. IHC (IgA, α chain specific). Bar = 10 µm. (E) Nasal tumor: CD20-positive neoplastic cells are located beneath the perineurium of a nerve bundle. IHC (CD20). Bar = 50 µm

immunopositivity was rare in the large lymphoid cells. Although a typical marginal zone pattern could not be confirmed in the examined lymph nodes, CD20-positive neoplastic cells were localized in the outer cortical area. Neoplastic cell invasion into the nerve bundles was clearly demonstrated by CD20 immunostaining (Fig. 2E).

Discussion

In the case described herein, the neoplastic tissue was histologically composed of lymphoid and plasmacytoid cells, and similar neoplastic cells were observed in a reported case of lymphoplasmacytic lymphoma (Fukunaga et al. 1993). However, in humans, plasmacytic differentiation may be observed in MALT lymphoma, which is characterized by marginal zone growth pattern, lymphoepithelial lesions, and blastic transformation to large-cell lymphoma (Isaacson et al. 2008). In diffuse large B-cell lymphoma, the main constituent tumor cells are larger than those in MALT lymphoma, and lymphoepithelial lesions are not detected. Because these features, except for the growth pattern, were ascertained in the present case, MALT lymphoma with large-cell transformation was suspected. The marginal zone growth pattern may have not been observed due to the advanced disease stage of this case. A diffuse growth pattern and loss of follicle-related architecture was observed at a late stage of development in the nodal marginal zone lymphoma of dogs, and some cases had a more aggressive clinical course (Cozzi et al. 2018). The turbinate mucosa was considered to be the primary site on the basis of the presence of lymphoepithelial lesions and the unique distribution of massive neoplastic lesions.

In general, IgM or IgG is produced in lymphoplasmacytic lymphoma in horses, cattle, and swine (Kadota et al. 1986, Nakajima et al. 1988, Fukunaga et al. 1993, Horiuchi et al. 1999, Murayama et al. 2011), whereas IgM expression is predominant in human lymphoplasmacytic lymphoma and MALT lymphoma (Feller & Diebold 2004b, Swerdlow et al. 2008). Because IgA plays an important role in mucosal immunity, the expression of cytoplasmic IgA supports the view that the present lymphoma is derived from an IgA-positive lymphocyte inhabiting the turbinate mucosa. In humans, the expression of μ rather than the γ heavy chain favors the diagnosis of lymphoma over plasmacytoma (McKenna et al. 2008). Because this horse was constitutionally weak, the prolonged nasal inflammation observed soon after birth may have subsequently led to the development of lymphoma. Similarly, many cases of human MALT lymphoma have a history of a chronic inflammatory disorder that results in the accumulation of extranodal lymphoid tissue.

Human MALT lymphoma is an indolent, locally aggressive disorder, and eradication of *Helicobacter pylori* using antibiotics results in its regression in many patients (Isaacson et al. 2008). In the horse in this study, nasal discharge was conspicuous at weaning, and the progression from chronic inflammation to lymphoma may have occurred at about this time. Systemic tumor cell infiltration may be associated with the advanced disease state in this case. Most equine B-cell lymphomas are classified as T-cell-rich large B-cell lymphomas or diffuse large B-cell lymphomas (Durham et al. 2013), which are included in the category of high-grade lymphoma in humans (Feller & Diebold 2004b). Some large B-cell lymphomas may result from the blastic transformation of low-grade lymphomas, including MALT lymphoma, as lymphomas are already progressed when diagnosed in horses.

Neurolymphomatosis, in which nerve bundles or plexuses are infiltrated by lymphoma cells, has been recorded in an equine T-cell-rich B-cell lymphoma (Westerman et al. 2014). Neurolymphomatosis is associated with immunodeficiency in humans; however, immunocompetent humans and animals can exhibit neurolymphomatosis without underlying etiology (Westerman et al. 2014). In the present case, the left orbital and upper jaw lesions were thought to result from neoplastic invasion from the adjacent left nasal mucosa, and the perineural and endoneural tumor spread may have occurred due to the presence of frequent neoplastic infiltrates in the nerve bundles. In addition, neoplastic replacement of the maxillary and mandibular muscles implies that lymphoma cells tend to diffusely infiltrate into loose tissues, such as the perimysium, rather than forming large tumor masses with compression of the surrounding tissues. In contrast, lymph node swelling and metastasis to parenchymal organs were inconspicuous, despite the animal being in the final stage of lymphoma. Accumulation of similar cases is needed for further study.

References

Cozzi, M. et al. (2018) Canine nodal marginal zone lymphoma: Descriptive insight into the biological behaviour. *Vet. Comp. Oncol.*, **16**, 246-252.

Durham, A. C. et al. (2013) Two hundred three cases of equine lymphoma classified according to the World Health Organization (WHO) classification criteria. *Vet. Pathol.*, **50**, 86-93.

Feller, A. C. & Diebold, J. (2004a) Extranodal lymphoma. *In* Histopathology of Nodal and Extranodal Non-Hodgkin's Lymphomas, 3rd ed., Springer, Berlin, pp. 186-363.

Feller, A. C. & Diebold, J. (2004b) Nodal B-cell lymphoma. *In* Histopathology of Nodal and Extranodal Non-Hodgkin's Lymphomas, 3rd ed., Springer, Berlin, pp. 19-120.

Fukunaga, K. et al. (1993) Lymphoplasmacytic lymphoma in a stallion. *J. Vet. Med. Sci.*, **55**, 465-467.

Horiuchi, Y. et al. (1999) An equine case of malignant lymphoma with numerous Russell bodies. *J. Jpn. Vet. Med. Assoc.*, **52**, 11-14 [In Japanese with English summary].

Hosokawa, S. et al. (2011) Head and neck MALT lymphoma. *Pract. Otol. (Kyoto)*, **104**, 47-53 [In Japanese with English summary].

Isaacson, P. G. et al. (2008) Extranodal marginal zone lymphoma of mucosa-associated lymphoid tissue (MALT lymphoma). *In* WHO Classification of Tumours of

Haematopoietic and Lymphoid Tissues, 4th ed., eds. Swerdlow, S. H. et al., International Agency for Research on Cancer, Lyon, pp. 214-217.

Jacobs, R. M. et al. (2002) Tumors of the hemolymphatic system. *In* Tumors in Domestic Animals, 4th ed., ed. Meuten, D. J., Iowa State Press, Ames, pp. 119-198.

Kadota, K. et al. (1986) Three types of swine immunoglobulin-producing tumours: lymphoplasmacytic lymphosarcoma, immunoblastic lymphosarcoma and plasmacytoma. *J. Comp. Pathol.*, **96**, 541-550.

McKenna, R. W. et al. (2008) Plasma cell neoplasms. *In* WHO Classification of Tumours of Haematopoietic and Lymphoid Tissues, 4th ed., eds. Swerdlow, S. H. et al., International Agency for Research on Cancer, Lyon, pp. 200-213.

Miglio, A. et al. (2019) Clinical and immunophenotypic findings in 4 forms of equine lymphoma. *Can. Vet. J.*, **60**, 33-40.

Muñoz, A. et al. (2009) Hematopoietic neoplasias in horses: myeloproliferative and lymphoproliferative disorders. *J. Equine Sci.*, **20**, 59-72.

Murayama, S. et al. (2011) Cytologic and immunophenotypic investigation of lymphohematopoietic neoplasms in cattle. *Jpn. Agric. Res. Q.*, **45**, 225-231.

Nakajima, H. et al. (1988) Lymphoplasmacytic lymphoma with cytoplasmic immunoglobulin-G in a pig. *Jpn. J. Vet. Sci.*, **50**, 835-837.

Swerdlow, S. H. (2008) Lymphoplasmacytic lymphoma. *In* WHO Classification of Tumours of Haematopoietic and Lymphoid Tissues, 4th ed., eds. Swerdlow, S. H. et al., International Agency for Research on Cancer, Lyon, pp. 194-195.

Valli, V. E. et al. (2006) Canine indolent nodular lymphoma. *Vet. Pathol.*, **43**, 241-256.

Wenzel, C. et al. (2003) Extranodal marginal zone B-cell lymphoma of mucosa-associated lymphoid tissue of the head and neck area; High rate of disease recurrence following local therapy. *Cancer*, **97**, 2236-2241.

Westerman, T. L. et al. (2014) Neurotropic T-cell-rich B-cell lymphoma in a 14-year-old Morgan gelding. *Can. Vet. J.*, **55**, 379-382.